Tryptophans in Membrane Proteins: Indole Ring Orientations and Functional Implications in the Gramicidin Channel†

W. Hu, K.-C. Lee, and T. A. Cross*

Department of Chemistry and Institute of Molecular Biophysics, Florida State University, Tallahassee, Florida 32306-3006

Received December 14, 1992; Revised Manuscript Received April 16, 1993

ABSTRACT: Orientational constraints generated from solid-state NMR of uniformly aligned gramicidin A in hydrated lipid bilayers have been used to determine the indole ring orientations for the four tryptophans of the gramicidin A monomer with respect to the bilayer normal and the channel axis. $^{15}N_{\epsilon 1}$ labeled tryptophan has been incorporated into gramicidin at positions 9, 11, 13, and 15. The chemical shift tensor orientation has been oriented with respect to the N–H bond via doubly labeled sample in which the $^{15}N_{\epsilon 1}$–^{1}H has been exchanged for ^{2}H. By observation of the dipolar coupled ^{15}N chemical shift powder pattern of the amino acid, σ_{cc} has been shown to be perpendicular to the plane of the ring and that σ_{aa} makes an angle of 25° with respect to the N–H bond. The indole ring orientations were obtained from a consideration of both the chemical shift and the ^{15}N–^{1}H dipolar interaction. These four rings have very similar orientations with respect to the bilayer normal as given by the range of angles between the bilayer and ring normals (64–67°). Furthermore, the N–H bond orientations with respect to the bilayer normal varies by only 10° among the four sites. This orientational analysis has been based on an assumption that large amplitude librational motions in the hydrated bilayer samples are not averaging the nuclear spin interactions. This assumption was verified by analyzing the ^{2}H quadrupole spectra of d_5-Trp_{11}-labeled gramicidin A in oriented preparations. The orientations predicted for the five C–H bonds in the indole ring from the ^{15}N data agreed (root-mean-square deviation of 3.7°) with the observed orientations from quadrupole splittings of the C–D bonds in the ring. From the orientation of the indole rings with respect to the bilayer normal and a polypeptide backbone conformation, the four typtophans of the gramicidin monomer are oriented with respect to the backbone of the channel conformation. The similarity among the indole orientations with respect to the bilayer normal is therefore consistent with the electrophysiological results that the individual replacement of the indole rings with phenyl rings results in a incremental decrease in the conductance of the channels formed. The indole orientations with respect to the backbone as defined by the side-chain torsion angles is not uniquely determined but yields a discrete set of possible values. The tryptophan orientation in the gramicidin model structure derived from solution NMR studies in SDS micelles is qualitatively if not quantitatively consistent with these solid-state NMR conclusions. The N–H orientations are consistent with the stabilizing influence of the indoles which has been speculated to result from hydrogen bond formation to the hydrophilic bilayer surface and possibly to the fatty acyl carbonyl oxygens. The dominant component of the dipole moment of each indole ring is parallel with the channel axis and oriented so as to lower the potential energy barrier for cation transit at the bilayer center. The radial component for the most likely indole conformers is oriented so as to stabilize the cation in the channel.

Tryptophan plays a fundamental role in membrane proteins. Uniformly oriented preparations of the polypeptide, gramicidin A, present a unique opportunity for studying, at very high resolution, the structure and dynamics of these residues by solid-state NMR.[1] The indole side chain has both hydrophobic and hydrophilic character, and consequently, it partitions at the hydrophobic–hydrophilic interface in lipid bilayers (Jacobs & White, 1989). In the few membrane proteins where a relatively high-resolution structure has been determined, tryptophans are frequently at the bilayer surface where they are oriented so that the indole N–H is directed toward the hydrophilic environment (Michel & Deisenhofer, 1990; Henderson, et al., 1990; Meers, 1990; Chattopadhyay & McNamee, 1991). Tryptophan may indeed play an important role in stabilizing membrane proteins through electrostatic interactions at the lipid bilayer surface. In some membrane proteins, such as porin, tyrosine seems to play a similar role where a ring of such residues on the exterior of the protein at the lipid–protein interface are directed toward the hydrophilic environment (Weiss et al., 1991). Gramicidin A has four tryptophan residues that are very important for the stability of the channel conformation and for its function. Recently, it has been suggested through computational (Meulendijks et al., 1989), electrophysiological (O'Connell et al., 1990), fluorescence (Scarlatta, 1991) and NMR (Lazo et al., 1992) studies that the indole N–H groups may hydrogen bond to the aqueous interface or directly to the lipid molecules. This appears to stabilize the gramicidin monomer in the bilayer leaflet (O'Connell et al., 1990). Furthermore, the indole possesses a substantial permanent dipole moment. The orientation of this dipole moment may have a significant effect on the ionic interactions of membrane proteins, and in this molecular system the tryptophan dipole moment appears to have a direct effect on the conductance of monovalent cations by the gramicidin channel.

Gramicidin A is a 15 amino acid polypeptide having the following sequence of alternating L and D amino acids: HCO-Val_1-Gly_2-Ala_3-$DLeu_4$-Ala_5-$DVal_6$-Val_7-$DVal_8$-Trp_9-$DLeu_{10}$-

† T.A.C. gratefully acknowledges the support of NIH Grant AI-23007.

* To whom correspondence should be addressed.

[1] Abbreviations: NMR, nuclear magnetic resonance; SDS, sodium dodecyl sulfate; Fmoc, 9-fluorenylmethoxycarbonyl; HPLC, high-performance liquid chromatography; DMPC, dimyristoylphosphatidylcholine.

0006-2960/93/0432-7035$04.00/0

Trp_{11}-$DLeu_{12}$-Trp_{13}-$DLeu_{14}$-Trp_{15}-NH-CH_2-CH_2OH. As a dimer, this extremely hydrophobic polypeptide forms a monovalent cation selective channel. In 1971 Urry proposed a novel structure, which was later called a β-helix because the backbone had β-sheet-type torsion angles and which was wound into a helical structure. The helix has a 4-Å-diameter pore and 6.3 residues/turn, such that the side chains are directed radially away from the channel which is lined with the amide linkages of the polypeptide backbone. Recently, the helix sense was determined to be right-handed from solid-state NMR derived orientational constraints (Nicholson & Cross, 1989). While this model for the folding motif of the channel is well-accepted, structural detail is absent. A crystallographic structural solution of the channel form has yet to be achieved despite the fact that cocrystals of gramicidin and lipid have been extant for years (Kimball & Wallace, 1981), but the most recent results from these crystals suggest a very different packing arrangement for the lipid and gramicidin than that of the native arrangement (Wallace & Janes, 1991). However, it is well known that gramicidin in a lipid bilayer is a single stranded helix (Katsaras et al., 1991). Arseniev and co-workers have determined the structure of a channel-like conformation in SDS micelles by solution NMR methods (Arseniev & Barsukov, 1986; Lomize et al., 1992). The folding motif is that of the channel state, in that it is a single-stranded helix with a right-handed helical sense and it forms a head-to-head dimer (amino terminus to amino terminus). However, there are numerous reasons why this structure must be used as a model of the channel state with caution. First the channel is a symmetrical dimer positioned such that the channel axis of one dimer is known to be parallel with the channel axis of the second monomer. In an extended bilayer the two parallel leaflets of the bilayer may help to maintain this structural feature. In SDS micelles these surfaces are curved and it is not clear that the monomer axes will be parallel, consequently distortions in the structure may be present at the monomer–monomer junction. The specific lipid–protein and monomer–monomer interactions suggested in this and other recent studies (Meulendijks et al., 1989; O'Connell et al., 1990; Scarlatta, 1991; Lazo et al., 1992) may be compromised by replacement of the lipid headgroup with a sulfate group. Phospholipid headgroups provide a relatively thick interfacial layer in which the hydrophilic part of tryptophan can be situated. In this region long-range ordering of the solvent is not possible because of the packing of the headgroups; consequently, an entropic ordering of the solvent in this region when a hydrophobic moiety is introduced is not possible. Recently, specific sidechain conformations in the bilayer bound channel state determined by solid-state ^2H NMR have been shown to be different from the Arseniev model (Killian et al., 1992). In fact, details determined by solid-state ^{15}N NMR of the backbone structure of the channel state, especially at the monomer–monomer junction differ significantly from the Arseniev model (Chiu et al., 1991; Mai et al., 1993). However, despite these predicted and observed differences in structural detail, the fold of gramicidin in SDS has clearly the same helical parameters as the channel state.

In gramicidin, the tryptophans have been recognized as functionally important for many years (Heitz et al., 1982). Gramicidin is biosynthetically produced by *Bacillus brevis* as a mixture of polypeptides. The conductance of gramicidin B (Phe_{11} replaces Trp_{11}) is substantially less than that of gramicidin A (Bamberg et al., 1976). In fact, if all of the tryptophans are replaced with phenylalanines the conductance is reduced by a factor of 20 (Becker et al., 1991). The effect of replacing the tryptophans one by one has an incremental effect on the conductance, and on the basis of this observation these authors have suggested that all of the tryptophans will have approximately the same orientation with respect to the channel axis. In this way the dipole moment for each of the tryptophans would be oriented in the same way and could modify the potential energy surface in an incremental way. Furthermore, when tryptophans are replaced by tyrosines, which also have a substantial dipole moment, the rate of conductance is not substantially affected. Upon replacement of tryptophans with phenylalanines or tyrosines, the backbone conformation, as assessed by ^{15}N chemical shifts in oriented samples, does not change (Fields, 1989). This chemical shift constraint is also sensitive to the amplitude of local motions for the specific site of interest, and consequently there does not appear to be any changes in either conformation or dynamics of the backbone upon aromatic amino acid substitution.

This study takes advantage of the orientational dependence of nuclear spin interaction tensors in samples that are remarkably well aligned with respect to the magnetic field (Cross et al., 1992). Isotopically labeled samples have been used so as to single out specific sites and nuclear spin interactions in the polypeptide in a lipid bilayer environment. From such sites oriented with respect to the field, the observed chemical shift can be interpreted as a constraint on how the spin interaction tensor is oriented with respect to the field, provided that the magnitudes of the tensor elements are known. Furthermore, if the tensor orientation is known with respect to the molecular frame then the orientation of the molecular frame is constrained with respect to the magnetic field. Finally, since the channel axis has been chosen to be parallel with respect to the magnetic field, then the molecular frame is constrained with respect to the channel axis. While tensor element magnitudes for the $^{15}N_{\epsilon 1}$ labeled tryptophan have been reported (Cross & Opella, 1983; Roberts et al., 1987) the tensor orientation for this site with respect to the molecular frame is experimentally defined here relative to the internuclear vector, the ^{15}N–^2H bond. To yield a unique orientation of the tensor with respect to the molecular frame it is assumed that one of the tensor elements is in the plane of the ring. This assumption appears to be reasonable based on the single crystal studies of amide peptide sites and histidine imidazole ring nitrogens (Harbison et al., 1981, 1984), as well as the magic angle spinning study of L-tryptophan·HCl (Roberts et al., 1987).

Three other nuclear spin interactions will be taken advantage of in this study. The ^{15}N–^1H and ^{15}N–^2H dipolar interactions have an axially symmetric tensor for which the magnitude can be readily calculated. Furthermore, the orientation of the unique tensor element is directed along the internuclear vector. The third additional interaction is the ^2H quadrupole interaction. Again this interaction for aromatic carbon bound deuterium is nearly axially symmetric and the unique axis is directed along the internuclear vector. The magnitude of the quadrupole interaction comes from aromatic model compounds (Kinsey et al., 1981).

The effort presented here is not the first effort by solid-state NMR to define the indole orientations of gramicidin A. Cornell and co-workers have presented ^{13}C data for each of the tryptophans labeled in the δ_1 site of the indole ring in oriented preparations of gramicidin containing bilayers (Cornell et al., 1988; Separovic et al., 1991). The authors impressively determined the orientation of the chemical shift tensor with respect to the N–C bond by taking advantage of

the $^{14}N_{\epsilon 1}$–$^{13}C_{\delta 1}$ dipolar interaction. Despite relatively small errors claimed by the authors, the data have been reported in two different papers with substantially different interpretations (±6 ppm) and complications associated with the relative magnitudes of the Zeeman and quadrupole interactions were ignored (Teng et al., 1992). Furthermore, not enough data were available to assess the local motions of the indole rings, thereby limiting their ability to derive detailed structural constraints. By ignoring potential local motions, the data were interpreted as consistent with the orientations of the indoles in Arseniev's model. Such an interpretation, while substantiating a published model is also consistent with conformations that have the opposite orientation for the N–H bond and dipole moment. These opposing orientations leave the functional questions unanswered. Consequently, an *a priori* determination of the orientations is needed for the channel state of gramicidin A in a hydrated phospholipid bilayer.

Once the indole orientations are determined relative to the channel axis their orientation in the plane of the bilayer can be restrained by considering the van der Waals contacts of the polypeptide backbone. With a limited set of conformations, the orientations of the dipole moments with respect to the channel are described.

METHODS AND MATERIALS

Sample Preparation. Gramicidin A samples isotopically labeled with $^{15}N_{\epsilon 1}$ Trp at position 9, 11, 13, or 15 were synthesized by solid-phase peptide synthesis with 9-fluorenylmethoxycarbonyl (Fmoc) chemistry (Fields et al., 1989). *N*-Fmoc-L-Trp($^{15}N_{\epsilon 1}$) was synthesized from Fmoc *N*-hydroxysuccinimide ester and $^{15}N_{\epsilon 1}$-L-Trp (Chang et al., 1980). The synthetic peptides were approximately 98% pure by reverse-phase HPLC analysis and were used for NMR studies without further purification.

Powder samples were prepared by cosolubilizing gramicidin A and DMPC at a molar ratio of 1:8 in organic solvent (5% ethanol in benzene). The solution was lyophilized to obtain the dry mixture. Hydrated samples were prepared by the addition of 40% (volume to total weight) HPLC-grade water to powder samples. After centrifugation, the samples were incubated for 2 weeks at 45 °C. Oriented samples were prepared by codissolving 30 mg gramicidin A and 90 mg DMPC (1:8 molar ratio) in 205 μL of HPLC grade methanol and 5 μL of HPLC grade water. The solution was kept at −5 °C overnight, and then 12.5 μL of this solution was spread on each of 20 glass coverslips (5.8 by 18 mm; 4 mm of length reserved for spacers). The samples on these coverslips were dried, and the coverslips were stacked in a square glass tube (6 by 6 by 19 mm). HPLC grade water was added to 50% (volume to total weight), and the tubing was sealed at both ends. The samples were incubated at 45 °C for approximately 3 weeks to achieve uniform hydration and orientation. Deuterium-exchanged $^{15}N_{\epsilon 1}$-L-Trp was obtained by refluxing a D_2O solution of Trp for 1 h at approximately pH 7. After lyophilization the indole amino proton of $^{15}N_{\epsilon 1}$-L-Trp was verified by ^1H NMR to be about 75% deuterated.

NMR Spectroscopy. The ^{15}N cross polarized spectra were recorded on a 400-MHz spectrometer built around a Chemagnetics data acquisition system (Chemagnetics Inc., Ft. Collins, CO). A home-built ^{15}N probe was used for observing both powder and oriented samples. The pulse width for a 90° flip angle was approximately 6 μs; a 2-ms mixing time was used for the deuterium-exchanged sample and 1 ms for all other samples. A Hahn echo with an interpulse delay of 180 μs was used to minimize probe ringing. A recycle delay of 7 s and a decoupling field of 55 kHz was typically used. ^{15}N–^1H separated local field spectra were obtained as in LoGrasso et al. (1989) and Teng et al. (1991) with a second dimension dwell time of 20 μs. All of the ^{15}N chemical shifts are reported relative to an external reference of a saturated solution of ^{15}N H_4NO_3.

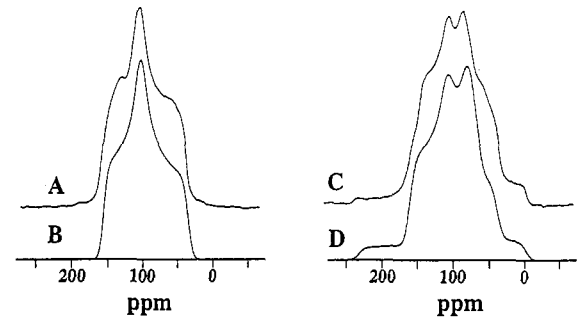

FIGURE 1: ^{15}N chemical shift powder pattern spectra of isotopically labeled tryptophan. (A) $^{15}N_{\epsilon 1}$-tryptophan, 6144 acquisitions. (C) ^2H-$^{15}N_{\epsilon 1}$-tryptophan, 12 624 acquisitions. (B) The spectral simulation of (A) yields tensor element magnitudes of $\sigma_{11} = 35$, $\sigma_{22} = 104$, and $\sigma_{33} = 158$ ppm. (D) The double labeled sample in (C) is only 75% deuterated as determined independently by solution NMR and consequently the spectral simulation reflects a 25% fraction of the signal that arises from sample that is not dipolar coupled. The tensor orientation is determined from this simulation to be $\alpha_D = 0°$ and $\beta_D = 25°$ where the definition of these angles are given in Figure 2.

Deuterium spectra were observed with a home-built single-channel probe using a resonant frequency of 61.5 MHz. A quadrupole echo pulse sequence (Davis et al., 1976) was used. Data were acquired with a dwell time of 1 μs, an interpulse delay of 30 μs, and a recycle delay of 1 s.

Data Processing. Spectra were processed on a Silicon Graphics Iris workstation with Felix software. ^{15}N chemical shift and ^{15}N–^2H dipolar coupled chemical shift powder pattern spectra were simulated with a modified version of the program TENSORI (Teng, 1990). These simulations were carried out on a Sun Sparc 1 workstation.

Molecular Modeling. Molecular modeling was carried out on a Silicon Graphics Iris workstation using the Insight II software package (Biosym Technologies, San Diego, CA). This software was used to view the 3D structure of various gramicidin channel models, to modify the peptide structures, and to output torsion angles, structural coordinates, and van der Waals contact violations. The χ_1 and χ_2 values of tryptophan for protein conformations obtained from the Protein Data Bank (Brookhaven) were also obtained using this software package.

RESULTS

Before the ^{15}N chemical shift interaction of the indole could be used as an effective orientational constraint the tensor orientation with respect to the molecular frame had to be determined. After the novel work of Hiyama et al. (1988) where they oriented the ^{15}N amide tensor in a dipeptide relative to the ^{15}N–^2H dipolar interaction, the indole ^{15}N site is here oriented with respect to the same dipolar interaction. Because the Zeeman interaction of the ^2H nucleus (61 MHz) is so much greater than the quadrupolar interaction (approximately 200 kHz) the quadrupolar effects on the ^{15}N resonance can be ignored. Consequently, the dipolar coupled (between spin 1 and spin $^1/_2$ nuclei) ^{15}N powder pattern spectra are calculated in much the same way as a spin $^1/_2$, spin $^1/_2$ dipolar-coupled spectrum with the exception that the ^2H nucleus has three spin states. Shown in Figure 1A is the ^{15}N spectrum of $^{15}N_{\epsilon 1}$-

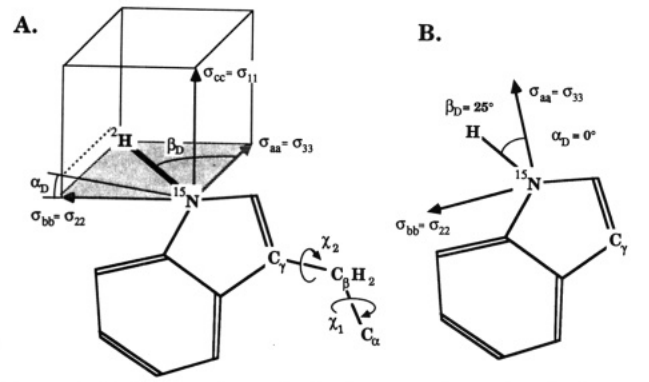

FIGURE 2: Definitions for angles in the tryptophan molecular frame. (A) The base plane of the cube is contiguous with the plane of the indole ring. A slight elevation of the ^{15}N–^{2}H bond is shown only to illustrate the definition of the α_D angle. (B) The orientation of the $^{15}N_{\epsilon 1}$ chemical shift tensor with respect to the molecular frame. $\sigma_{11} = \sigma_{cc}$ is perpendicular to the plane of the ring; $\sigma_{33} = \sigma_{aa}$ is at a 25° angle to the N–H bond and; $\sigma_{22} = \sigma_{bb}$ completes the orthogonal coordinate system by making an angle of 65° with respect to the N–H bond.

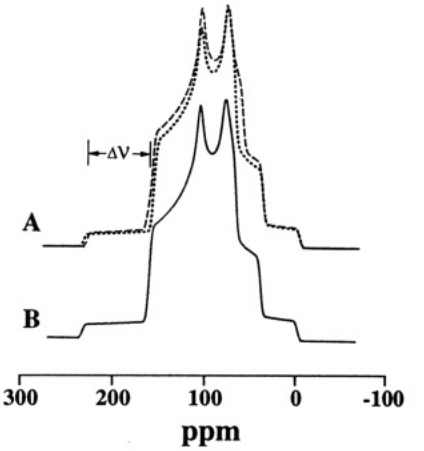

FIGURE 3: This figure illustrates the sensitivity of the powder pattern line shape for the determination of β_D as presented in Figure 1. the singularities of these powder pattern spectra can be determined with an error of ±1.5 ppm. The dipolar splitting, $\Delta\nu$ around the σ_{33} tensor element is particularly sensitive to β_D. (A) The dashed line represents a β_D angle of 30° while the dotted line an angle of 20°. The difference in $\Delta\nu$ when β_D differs by 6° (22° and 28°) is 4.5 ppm. Consequently, the error bar in the determination of β_D is less than ±3°. (B) the solid line represents the same spectral parameters as in Figure 1D with less line broadening.

labeled tryptophan in which the tensor element magnitudes are obtained by spectral simulation (Figure 1B) resulting in $\sigma_{33} = 158$, $\sigma_{22} = 104$ and $\sigma_{11} = 35$ ppm. In Figure 1C an ^{15}N spectrum of the N-deuterated amino acid is shown in which the sample has been 75% deuterated as determined by solution NMR. By using the tensor element magnitudes as known values the only remaining variables are the α_D and β_D polar angles that orient the ^{15}N chemical shift tensor with respect to the unique axis of the dipolar interaction that lies along the ^{2}H–^{15}N vector (Figure 2A). Following ^{15}N tensor element determinations from single-crystal studies, such as amide polypeptide backbone sites (Harbison et al., 1984) and the histidine ring nitrogens (Harbison et al., 1981), it is assumed here that a tensor element ($\sigma_{aa} = \sigma_{33}$) lies in the molecular plane. The *aa*/*bb*/*cc* nomenclature for the tensor elements represent definitions with respect to the molecular frame rather than with respect to the frequency magnitudes in the powder spectra (Wang et al., 1992; Teng et al., 1992). These definitions avoid ambiguities in comparing tensor orientations from one molecule or molecular site to another where η is near the extrema of its range, i.e., near either 1 or 0. Here the definitions are similar to those described previously for the amide ^{15}N sites (Teng et al., 1992). σ_{cc} is approximately perpendicular to the indole plane, σ_{aa} lies in the $C_{\delta 1}NH$ bond angle and σ_{bb} completes the orthogonal coordinate system. The spectral simulation shown in Figure 1D results in σ_{cc} being perpendicular ($\alpha_D = 0$) to the plane of the aromatic ring and the N–H bond makes an angle of 25° with the σ_{aa} axis as shown in Figure 2B. An α_D angle of 0° was anticipated since one of the tensor elements for each of the histidine nitrogens and numerous amide nitrogens have been shown to be perpendicular to the molecular plane. Figure 3 shows the sensitivity of the powder pattern simulations to the angle β_D. This angle is, in general, quite variable and for this indole site it has previously been assumed to be zero (Cross & Opella, 1983). This ^{15}N data clearly shows that β_D has a significant angle of 25°. As indicated in Table I the determination of the chemical shift tensor element magnitudes has an error of ±1.5 ppm. In Figure 3 dashed and dotted simulation lines are drawn for a variation of β_D of ±5° yielding a $\Delta\nu$ variation in spectral discontinuities that is much greater than 3 ppm. Even a β_D variation of ±3° results in a change of $\Delta\nu$ of 4.5 ppm; consequently, the error in β_D is less than ±3°.

The second consideration prior to a structural interpretation of the observed spin interactions is to consider the dynamics of the molecular system in the channel state. Gramicidin in a hydrated lipid bilayer rotates about an axis parallel with the bilayer normal (Smith & Cornell, 1986; Fields et al., 1988) resulting in axially symmetric interactions such that the unique axis of all the spin interactions is parallel with respect to the bilayer normal. Figure 4 shows a comparison of powder pattern spectra for $^{15}N_{\epsilon 1}$-Trp$_9$-labeled gramicidin A. In Figure 4A the spectrum of a dry powdered sample of gramicidin A represents the static chemical shift tensor, while the room temperature spectrum of gramicidin A in hydrated lipid bilayers (Figure 4B) shows the averaging due to the uniaxial global rotation of the channel. The conversion from axial asymmetry in the static preparation to axial symmetry via rotation about the bilayer normal is clearly shown. From spectra similar to that presented in Figure 4A the magnitudes of the tensor elements have been determined for each individual tryptophan in gramicidin A (Table I). In Figure 4C a spectrum of an oriented preparation is presented. The observed frequency is that of $\sigma_\parallel$ because the bilayer normal has been placed parallel with respect to the magnetic field and the motional axis is parallel with respect to the bilayer normal. These observed chemical shifts from oriented samples are presented in Table I.

Once the tensor element magnitudes are determined for each site of interest in gramicidin and the orientation of the tensor determined from doubly labeled samples of the amino acid, the critical remaining question concerns the magnitude of local motions. By first assuming that these motions are restricted to small amplitudes so that the tensor elements are not significantly averaged, the data from oriented samples can be interpreted to yield the orientation of the covalent bonds in the indole ring. For the Trp$_{11}$ site two independent data sets can be used (^{15}N and ^{2}H) to define the bond orientations of the indole ring. Each data set is based on tensors having a different orientation with respect to the molecular frame; consequently, anisotropic motions would affect these tensors differently and the resultant bond orientations would be substantially different. Local motions of amino acid side chains must be anisotropic if the polypeptide backbone to which the side chains are tethered is undergoing anisotropic motions, as is the situation here for the channel

Table I: ^{15}N NMR Data from Four Specific Site-Labeled Gramicidin A Preparations

	Trp_9	Trp_{11}	Trp_{13}	Trp_{15}
$^{15}N_{\epsilon 1}$–H splitting(kHz)[a]	13.2 ± 1.0	11.1 ± 1.0	10.1 ± 2.0	7.7 ± 1.0
N–H orientation (deg)	32, 148	36, 144	37, 143	42, 138
^{15}N obs chem shift (ppm)[a]	145 ± 1	144 ± 1	144 ± 1	139 ± 1
σ_{11}, σ_{22}, σ_{33} (ppm)[b]	36, 112, 164 ± 1.5	35, 114, 168 ● 1.5	35, 115, 167 ● 1.5	37, 117, 166 ● 1.5
θ_{11} (deg)	67, 113	65, 115	65, 115	64, 116
θ_{22} (deg)	88, 92	91, 89	93, 87	98, 82
θ_{33} (deg)	23, 157	25, 155	25, 155	28, 152

[a] Obtained from uniformly oriented gramicidin A in hydrated DMPC lipid bilayers. [b] Tensor elements obtained from dry powder samples of gramicidin A with DMPC.

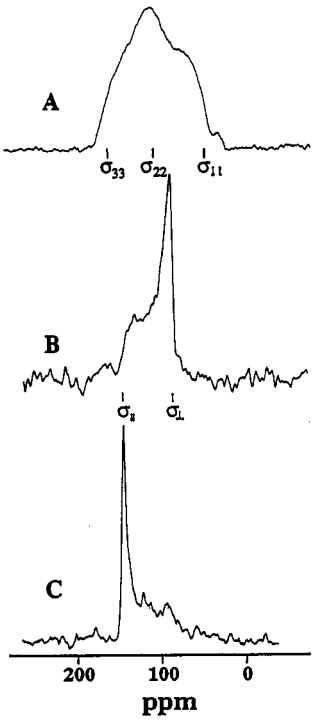

FIGURE 4: ^{15}N chemical shift spectra of $^{15}N_{\epsilon 1}$-Trp_9 labeled gramicidin A. (A) Static powder pattern spectrum obtained from a dry preparation, 11 888 acquisitions. Consequently the tensor is asymmetric and characterized by three elements: σ_{11}, σ_{22}, and σ_{33}. (B) Sample in a hydrated lipid bilayer above the phase transition showing averaging of the asymmetric tensor to an axially symmetric tensor, characterized by $\sigma_\parallel$ and $\sigma_\perp$, obtained with 896 acquisitions. (C) When the motional axis (parallel with the bilayer normal and the channel axis) is aligned parallel with respect to the magnetic field then the observed resonance is a sharp line at the $\sigma_\parallel$ frequency, obtained with 8944 acquisitions.

conformation of gramicidin in a lipid bilayer (Nicholson et al., 1989, 1991). For an indole ring, in addition to the global motions and the small amplitude librational motions of the backbone, there are only two degrees of motional freedom described by the χ_1 and χ_2 torsion angles (Figure 2) and the torsional motions about these angles. χ_1, in particular, is known to be highly constrained by van der Waals contacts (McGregor et al., 1987). Anisotropic local motions will average the nuclear spin interaction tensors around the indole ring differentially depending on the tensor element orientations with respect to the motional axis or axes.

As will be described below, based solely on the ^{15}N–^1H dipolar interaction and the ^{15}N chemical shift the orientation of the indole rings with respect to the magnetic field can be determined. From this orientation for the Trp_{11} site it is possible to predict the orientation of the C–H bonds in the indole ring for comparison with ^2H data for each of these sites (Table II). The ^2H spectrum of d_5-Trp_{11} labeled gramicidin A is shown in Figure 5. Five quadrupole splittings are readily

Table II: Trp_{11} Orientation with Respect to the Magnetic Field. Comparison of Calculated C–D Bond Orientations Based on ^{15}N Spectroscopy and the Observed C–D Orientations from Deuterium Quadrupole Splittings

	$C_{\delta 1}$-D	$C_{\epsilon 3}$-D	$C_{\zeta 3}$-D	$C_{\eta 2}$-D	$C_{\zeta 2}$-D
^2H study					
quadrupole splitting(kHz)	77.2	42.5	192	−99	38.9
bond orientation (deg)	44	131	153	108	49
^{15}N study					
bond orientation (deg)	46	127	148	110	53
orientation difference (deg)	−2	4	5	−2	−4

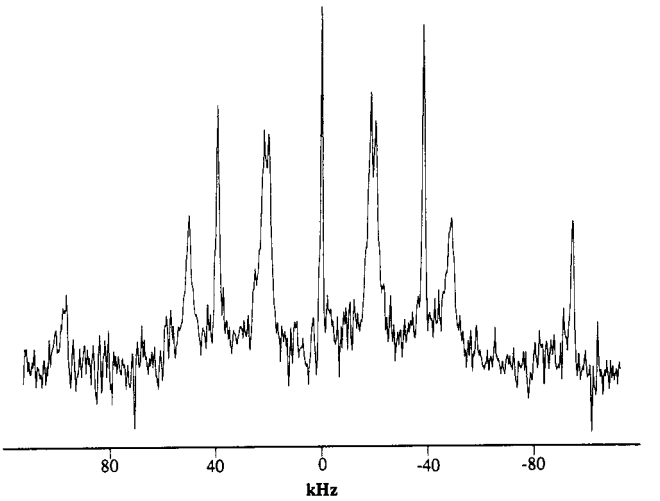

FIGURE 5: ^2H NMR spectrum of d_5-Trp_{11} gramicidin A in an oriented lipid bilayer preparation obtained with 24 800 acquisitions. The maximal quadrupole splitting, assuming no motional averaging is 274 kHz. Five quadrupole splittings are resolved and a small amount of residual HDO is observed at the spectral center. The observed splittings and their direct interpretation is given in Table II.

apparent and residual HDO at the carrier frequency. For Table II these quadrupole splittings were interpreted using a quadrupole interaction of 183 kHz (e^2qQ/h; Kinsey et al., 1981). The tensors for C–D bonds are oriented such that the unique axis of the interaction tensor is aligned parallel with the C–D bond, and it is assumed here that the ^2H tensor is axially symmetric. The assignments for the quadrupole splittings are readily achieved. Since the $C_{\zeta 2}$–D and $C_{\epsilon 3}$–D bonds are virtually parallel with respect to each other the two similar quadrupole splittings, 38.9 and 42.5 kHz are assigned to these two sites. The largest splitting is +192 kHz and can represent only the ζ_3 deuteron based on the ^{15}N determined orientation of the indole ring and the fact that motional averaging will only reduce the magnitude of this splitting. The next largest splitting is 99 kHz and is consistent with only the orientation of the η_2 deuteron. This leaves the 77-kHz splitting to be assigned to the δ_1 deuteron. These observed splitting values and those predicted from the ^{15}N based orientation are presented in Table II. Since the bond orientations from the two sets of data are very similar (root-

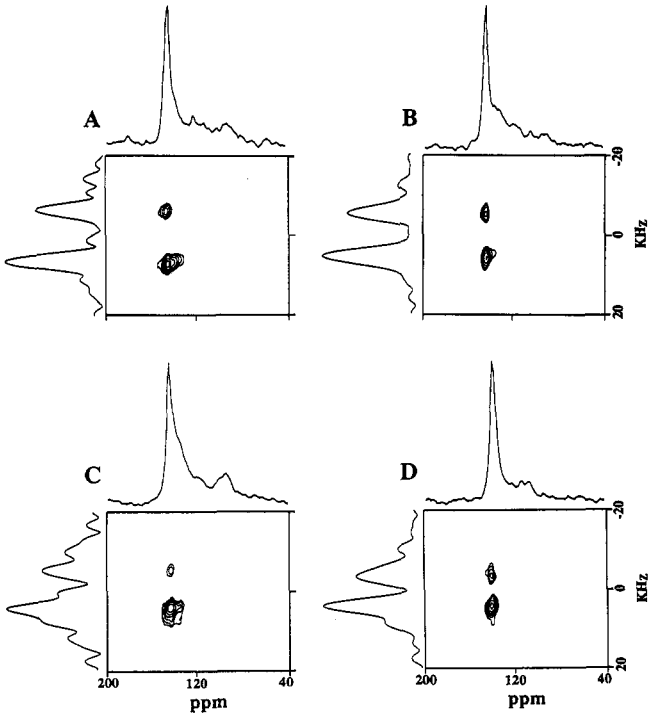

FIGURE 6: Separated local field spectra of $^{15}N_{\epsilon 1}$-Trp labeled gramicidin A in uniformly aligned lipid bilayers that are fully hydrated at room temperature. Typical number of acquisitions for these four data sets is 700 for each of 16 t_2 values. A chemical shift spectrum is displayed at the top of each figure and a slice through the dipolar dimension at the resonant chemical shift is shown to the left of each figure. (A) Trp_9-labeled gramicidin. (B) Trp_{11}-labeled gramicidin. (C) Trp_{13}-labeled gramicidin. (D) Trp_{15}-labeled gramicidin.

mean-square deviation of 3.7°), then our initial assumption that the local motional amplitudes are small is verified.

Figure 6 shows the separated local field spectra of the four tryptophan sites and in Table I the dipolar splittings and observed chemical shifts are presented from these oriented samples. We have shown previously (LoGrasso et al., 1989) that for calculating the magnitude of the dipolar interaction ($\nu_\parallel = h\gamma_N\gamma_H/r^3$) the bond length is best chosen to be that of the neutron diffraction bond length. While there is no neutron study of trytophan or indole the neutron bond length from amide peptide studies (1.024 Å; Kvick et al., 1977) has been used here. These results and those of LoGrasso et al. (1989) continue to contrast with magic angle spinning results where very large vibrational amplitudes were imposed to account for the reduced dipolar interactions that were observed by MAS and homonuclear decoupling methods (Roberts et al., 1987). The dipolar splittings in oriented samples ($\Delta\nu_{obs}$) are interpreted via the following expression:

$$\Delta\nu_{obs} = \nu_\parallel(3\cos^2\theta_H - 1) \quad (1)$$

where θ_H is the angle between the magnetic field direction and the dipolar vector. Consequently, the range for the dipolar splitting is from $2\nu_\parallel$ to $-\nu_\parallel$. We are unable to determine the sign of the dipolar splittings when the observed value is between $+\nu_\parallel$ and $-\nu_\parallel$, and this leads to an ambiguity in the determination of θ_H. Another source of ambiguity arises because the sign of cos θ is undetermined. Therefore, for each observed dipolar splitting two or four possible orientations for the N–H bond are achieved. These orientations are referred to here as orientational constraints.

The static ^{15}N chemical shift tensor is axially asymmetric, consequently the orientation of each tensor element must be defined rather than the orientation of the single unique tensor

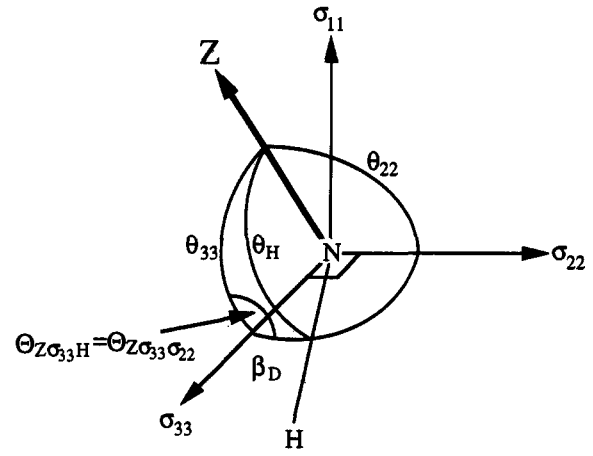

FIGURE 7: Use of spherical trigonometry to solve the orientation of bonds in the plane of the indole ring. The orientation of the tensor elements, σ_{22}, σ_{33}, and $\nu_\parallel$ is shown with respect to the magnetic field direction, the Z axis.

element as was done for the dipolar interaction:

$$\sigma_{obs} = \sigma_{11}\cos^2\theta_{11} + \sigma_{22}\cos^2\theta_{22} + \sigma_{33}\cos^2\theta_{33} \quad (2)$$

here cos θ_{ii} represents the direction cosines that orient the tensor elements, σ_{ii}, with respect to the magnetic field and σ_{obs} is the observed chemical shift for a sample that has been aligned so that all molecules have the same orientation with respect to the magnetic field direction. Since the chemical shift tensor element magnitudes, σ_{ii}, have been determined and σ_{obs} is measured, only the direction cosines remain unknown, however:

$$\sum_{i=1}^{3}\cos^2\theta_{ii} = 1 \quad (3)$$

Consequently, there are two equations and three unknowns. Because the orientation of this tensor is known with respect to the molecular frame it is possible to convert the σ_{obs} into an orientational constraint, albeit one in which the solution set is larger than for the dipolar or quadrupolar interaction. Furthermore, the sign of the direction cosines are once again undetermined. The orientational constraint for the tryptophans can be used in two ways. First, the NMR observables (^{15}N chemical shift and ^{15}N–^1H dipolar splitting) can be calculated from model structures and compared to the experimentally observed values. Second, the orientational constraints can be combined with covalent and steric constraints from the macromolecule (Brenneman & Cross, 1990; Teng et al., 1991). For this latter option, by combining the NMR observables, discrete orientations result for the chemical shift tensor elements with respect to the magnetic field. Two of these tensor elements are located in the indole plane (Figure 2) and consequently, from spherical trigonometry and Figure 7 eqs 4 and 5 follow:

$$\cos\theta_H = \cos\theta_{33}\cos\beta_D + \sin\theta_{33}\sin\beta_D\cos\Theta_{Z\sigma 33H} \quad (4)$$

$$\cos\theta_{22} = \cos\theta_{33}\cos 90° + \sin\theta_{33}\sin 90°\cos\Theta_{Z\sigma 33\sigma 22} \quad (5)$$

θ_H and β_D are known values and $\Theta_{Z\sigma 33H}$ and $\Theta_{Z\sigma 33\sigma 22}$ are two equal spherical angles. By combination of these two equations with eqs 2 and 3, θ_{33}, θ_{22} and θ_{11} can be determined. In a similar way these mathematical techniques can be applied for the determination of all bond orientations in the indole plane including the C_β–C_γ bond. For this purpose the covalent geometry of tryptophan in an oligopeptide was taken from Subramanian and Sahayamary (1989). This procedure

Table III: Comparison of Model-Based Predictions of ^{15}N Chemical Shifts and ^{15}N–^{1}H Dipolar Splittings with Observed Results for the Gramicidin Channel Conformation of the Backbone

	Trp_9[a]	Leu_{10}[a]	Trp_{11}[a]	Leu_{12}[a]	Trp_{13}[b]	Leu_{14}[b]	Trp_{15}[a]
^{15}N chemical shift (ppm)							
observed[c]	198	144	185	132	182	131	181
predicted	194	148	182	133	180	129	179
^{15}N–^{1}H dipolar splitting (kHz)							
observed[d]	20.7	13.5	20.9	16.2	20.9	14.3	20.9
predicted	21.3	18.3	22.1	16.6	20.8	13.4	22.3
bond directions (deg)[e]							
$\theta_{Z\alpha N}$	120		119		118		112
$\theta_{Z\alpha\beta}$	107		108		102		112

[a] Structure model of Professor Roux. [b] Structure model of Professor Arseniev. [c] Data from Mai et al. (1993). [d] Data from Ketchem and Cross (unpublished). [e] The bond directions were calculated from coordinates of the monomer in which the helix progresses along the positive Z axis from N to C terminus.

generates the detailed orientation of the Trp rings with respect to the magnetic field direction and the channel axis. Only two possible orientations of the aromatic rings relative to the channel axis remain, characterized by cos θ_H (Table I). Structural order in the plane of the bilayer can be achieved via a consideration of the geometrical constraints imposed by the short tether of the tryptophan side chain to the polypeptide backbone. The conformational flexibility of the tryptophan side chains is characterized by the torsion angles, χ_1 and χ_2, that describe the sidechain conformation relative to the polypeptide backbone. To determine these angles, bond orientations in the polypeptide backbone need to be assumed from computed or experimental models, because the three dimensional structure of the gramicidin channel in a lipid bilayer environment has not been experimentally determined.

The appropriate backbone orientations can be chosen for each site by comparing observed ^{15}N chemical shifts and the ^{15}N–^{1}H dipolar splittings with predicted values from a variety of model structures that have been provided by research groups performing molecular dynamics computations on the gramicidin channel. In this way it has been possible to choose a model that fits the observed backbone data (Mai et al., 1993; Ketchem & Cross, unpublished) for each tryptophan backbone site (Table III). The backbone conformations provide the remaining bond orientations (C_α–N and C_α–C_β) necessary for the definitions of the sidechain torsion angles, χ_1 and χ_2. Such calculations of the torsion angles can be achieved by using spherical trigonometry. By definition the torsion angle, χ_1, values can be calculated according to the following equation (Brenneman & Cross, 1990; Teng et al., 1991):

$$\chi_1 = \pm(\Theta_2 \pm \Theta_1) \qquad (6)$$

using the angle definitions given in Figure 8. While this expression yields four potential χ_1 values, only two of these are consistent with the NMR data. Similarly, expressions can be developed for χ_2 and for a given χ_1 value only two values for this torsion angle are consistent with the NMR data. A purely analytical analysis of the number of possible torsion angles can be conducted and confirms the result of two χ_1 and two χ_2 angles. Therefore, for each indole orientation with respect to the Z axis, four orientations relative to the polypeptide backbone can be calculated. As stated before, two possible indole orientations relative to the bilayer normal and channel axis exist and consequently eight possible χ_1/χ_2 pairs exist for each of the tryptophans in gramicidin A. These values are presented in Table IV.

The ambiguity with respect to the bilayer normal and the channel axis can be eliminated by considering the specific χ_1 and χ_2 values for each of the tryptophans. Many studies have shown that the χ_1 values for Trp in X-ray crystallographic

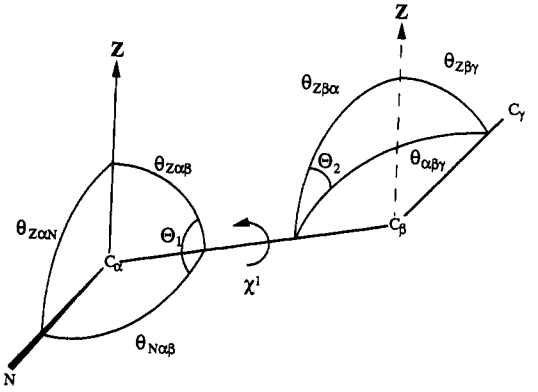

FIGURE 8: Use of spherical trigonometry to solve for χ_1 and χ_2 torsion angles. Angles $\theta_{Z\beta\alpha}$ and $\theta_{Z\alpha\beta}$ represent complements to each other. The angles involving the Z axis are either experimentally determined or experimentally verified. The angles between adjacent bonds are dictated by the covalent geometry. Θ_1 and Θ_2 represent angles on the surface of a sphere.

Table IV: Development and Refinment of χ_1 and χ_2 Values (deg) for Each Tryptophan Residue[a]

	solid-state NMR result			Arseniev's model		
	$N_{\epsilon 1}$–H orientations (obs)	χ_1	χ_2	$N_{\epsilon 1}$–H orientations	χ_1	χ_2
Trp_9	**32**[b]	**177**	**28, 82**	26	167	89
	32	**278**	**278, 332**			
	148	116	235, 289			
	148	339	71, 125			
Trp_{11}	**36**	**172**	**28, 86**	34	295	307
	36	**283**	**274, 332**			
	144	123	228, 282			
	144	334	78, 132			
Trp_{13}	**37**	**172**	**40, 93**	37	292	270
	37	**295**	**267, 320**			
	143	126	238, 292			
	143	341	68, 122			
Trp_{15}	**42**	**173**	**29, 85**	45	291	268
	42	**295**	**275, 331**			
	138	136	224, 280			
	138	332	80, 136			

[a] Backbone conformation for Trp_9, Trp_{11}, and Trp_{15} is from Roux's model. Backbone conformation for Trp_{13} is from Arseniev's model. These represent the best fit backbone conformations to the solid state NMR data. [b] Boldface represents potential conformations following refinement.

structure determination of proteins are near the three rotameric $\chi_1 = 60°$, 180°, and 300° states (Janin et al., 1978; Bhat et al., 1979; Ponder & Richards, 1987; McGregor et al., 1987). At the same time, the absence of χ_1 values around 0°, 120°, and 240° for the aromatic amino acids has been noted (McGregor et al., 1987).

To analyze more precisely the χ_1 distributions of tryptophan in proteins, 91 χ_1 and χ_2 values for Trp from 30 high-resolution

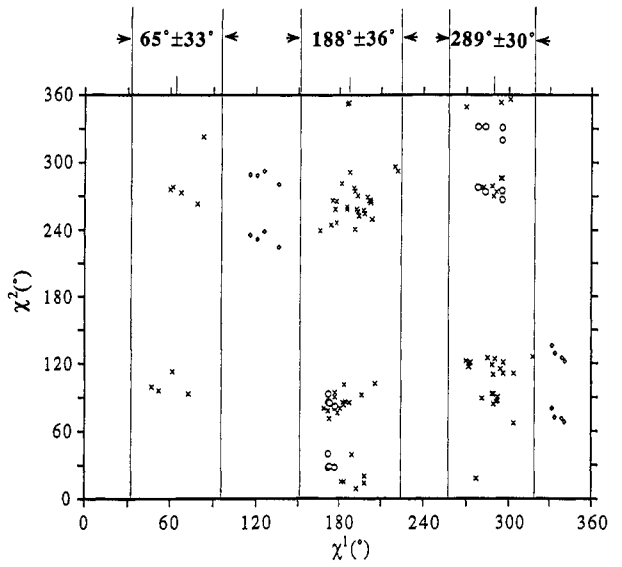

FIGURE 9: χ_1 and χ_2 angles for tryptophan orientations in 30 high resolution (<1.5-Å resolution) structures are marked with an ×. χ_1 is highly restrained being limited to only 55% of the orientational space for 99.7% of the conformer population. A plot of possible (◇ and ○) χ_1 and χ_2 angles for each of eight tryptophan conformations and each of the four gramicidin indoles is shown. The ◇ possibilities lie outside the 99.7% standard deviation boundaries and are not discussed further. The remaining indole conformations fall within the 180 and 300° χ_1 rotameric conformational regions. Two of the four remaining clusters have χ_2 values similar to the ±90° torsional angles suggested by the Raman studies (Takeuchi et al., 1990).

(0.8–1.5 Å) protein X-ray structures were collected. All of these protein structures came from the Protein Data Bank (Brookhaven) except for one gramicidin crystal structure (Langs et al., 1991) that David Langs has generously provided. The χ_1 and χ_2 values were calculated from the protein coordinates using Biosym software. For the proteins containing multiple subunits, the χ_1 and χ_2 values were counted only if they were different for the separate subunits. The mean value and three times the standard deviation for the χ_1 distribution are shown in Figure 9. The mean values are very close to earlier results (Janin et al., 1978; McGregor et al., 1987), but the standard deviations are substantially smaller, presumably resulting from the use of very high-resolution crystal structures while Janin's study used structures from diffraction data having a resolution as low as 2.5 Å. The χ_1 values calculated in this study for gramicidin having the $N_{\epsilon 1}$–H oriented toward the channel center ($\theta_H > 90°$) are well outside the standard deviation boundaries (99.7% of the population) of the rotameric states. In fact, these unrealistic conformations show the C_β–C_γ bond eclipsed with the amino group or carbonyl group of the polypeptide backbone. On the other hand, the χ_1 values for the Trp conformations having the $N_{\epsilon 1}$–H bond oriented toward the bilayer surface ($\theta_H < 90°$) are very close to the mean values for the $\chi_1 = 180°$ and 300° conformations. Consequently, this analysis limits the indole orientations to a unique orientation with respect to the channel axis and a set of four orientations for each of the tryptophans relative to the polypeptide backbone.

DISCUSSION

The tensor orientation shown here for the indole ^{15}N site represents a unique tensor characterization for tryptophan. Prior to this the molecular symmetry axis frame has been assumed for the chemical shift tensor orientation in which σ_{11} ($= \sigma_{cc}$) is perpendicular to the indole plane and σ_{33} ($= \sigma_{aa}$) is aligned with the N–H bond (Cross & Opella, 1983). This orientation had been experimentally verified by magic angle spinning correlation of the ^{15}N chemical shift and ^{15}N–^1H dipolar interactions (Roberts et al., 1987). Furthermore, the orientations for the ^{15}N tensors in histidine (Harbison et al., 1981) are in qualitative agreement with the results reported here. $\sigma_{11} = \sigma_{cc}$ is perpendicular to the imidazole plane as in the tensors mentioned above, and also for the numerous amide ^{15}N tensors that have been determined (Oas et al., 1987; Hartzell et al., 1987; Teng & Cross, 1989; Teng et al., 1991; Hiyama et al., 1988). The β_D angle is the variable angle in amide tensors resulting in a range of orientations for the $\sigma_{33} = \sigma_{aa}$ axis with respect to the N–H bond. In such studies, Munowitz et al. (1982) showed that this angle for glycylglycine hydrochloride monohydrate was 25 ± 5°. Later Harbison et al. (1984) derived an angle of 21° for this same molecule from a high-resolution single crystal study. In other early studies of amide sites by Cross and Opella (1985) it appeared reasonable, if not necessary, to choose the molecular symmetry axis frame for the tensor orientation, because there was every reason to believe that crystal packing forces would distort tensor element magnitudes and orientations. In part, this concern has been elegantly justified by the work by Hiyama et al. (1988) in which two crystal forms of the same peptide yield vastly different tensor element magnitudes. Now, with the advent of determining the tensor orientation *in situ* for the site of interest (Teng & Cross, 1989; Teng et al., 1992; Wang et al., 1992) it is no longer necessary to make such assumptions for the orientation of the tensor. Angles between σ_{aa} and the N–H bond have been achieved by Oas et al. (1987) and Mai et al. (1993) for other ^{15}N glycine containing peptides that are in the range 20–22°. Because the NHC_1 bond angle is smaller in other peptides (Fletterick et al., 1971) and the β_D angle is greater for non-glycyl sites (Hartzell et al., 1987; Teng & Cross, 1989; Teng et al., 1992; Mai et al., 1993) this angle has been shown to be as small as 12°. Therefore, it is clear that the angle between the N–H bond and the σ_{aa} axis is typically nonzero and in the range 9–22° (9°: $^{15}N_2$ of histidine, Harbison et al. (1981); 22°: ^{15}N Gly_2 gramicidin A, Mai et al. (1993)). For tryptophan the angle between σ_{aa} and the N–H bond is 25° and represents a slight extension for this range of angles. This result is significantly at variance with the Roberts et al. (1987) study of L-tryptophan·HCl in which β_D was observed to be 0°. While it is advantageous to use tensor orientations determined *in situ*, the orientation of a tensor determined from model compounds, such as the amino acid, tryptophan, provides us with an approximation of the tensor orientation prior to having the full tensor characterization for each separate indole site in the gramicidin channel conformation. Such characterizations will have to await further refinement efforts.

It is clear from the self-consistent data for Trp_{11} which overdetermines the orientation of this indole ring that for this residue local motion amplitudes are indeed small and that the determined ^{15}N chemical shift tensor orientation is approximately correct. An indication of the sensitivity of the quadrupole splitting to orientation is illustrated by two observations. The line widths of the δ_1 resonances are only 1.4 kHz in breadth (Cross et al., 1992). If this width at half-height is interpreted as due to a range in orientation for this site, then these specific C–D bonds throughout this sample are oriented within a Gaussian range of ±0.2°. Furthermore, it is known from the elegant spectra of Hing et al. (1990) that these lines can be further narrowed by ^1H decoupling. The second indication of orientational sensitivity is a partial but very accurate determination of the covalent geometry in this

ring. If it is reasonably assumed that the ^2H electric field gradient tensor has the same orientation with respect to the molecular frame for the $\zeta 2$ and $\epsilon 3$ sites, then the different splittings can be interpreted as a difference in orientation, not only with respect to the field but with respect to each other. The 3.6 kHz difference dictates a $0.50 \pm 0.10°$ orientational difference between these two bonds. Not only can NMR be used to very accurately determine bond lengths (Pake, 1948; DiVerdi & Opella, 1982; Cross & Opella, 1982; Roberts et al., 1987; LoGrasso et al., 1989), but here it is shown that relative bond orientations can also be determined with very high precision even for a polypeptide in an noncrystalline environment.

Because of the very good agreement of the predicted and observed quadrupole splittings, the amplitude of local motions for the indole rings is estimated to be small. This is consistent with an estimated gel-phase local librational amplitude of 5–15° from unoriented ^2H quadrupolar spectra (Macdonald & Seelig, 1988) and with a liquid-crystal phase computational estimate by Meulendijks et al. (1989) of a highly restrained residue. Further support for this concept comes from evidence that these indole N–H groups form hydrogen bonds (Lazo et al., 1992). Potentially, these hydrogen bonds could be to the lipid headgroup or to the fatty acid carbonyl oxygens (Meulendijks et al., 1989; O'Connel et al., 1990). These hydrogen bonds are not expected to be long-lived as the overall correlation time for the channel has been estimated to be 200 ns (Macdonald & Seelig, 1988) and boundary lipid exchanges with bulk lipid at a rate much greater than 10^6 s^{-1} time scale. We have assumed here that the local motional amplitudes are similar for the four tryptophan sites, because the structural constraints are all so similar. This lack of distinguishable boundary lipid caused Seelig and Macdonald (1987) to suggest that either the gramicidin surface is very fluid or that the surface is very irregular, allowing the lipid to occupy a wide range of conformational space. It has been shown here that the tryptophans are relatively rigid and therefore the channel exterior is not highly fluid. The irregularity of the channel surface with the lipid is not known without a final resolution of the side-chain torsion angles.

By utilizing spherical trigonometry it has been possible to take maximum advantage of the nuclear spin interaction constraints. For the field of structural biology these are unusual constraints. As shown here, the precision for the determination of the ^2H quadrupole splittings is very high especially when considered in orientational space. The accuracy of the interpretation is limited by knowledge of the ^2H tensor. Solid-state NMR is beginning to provide a few very high resolution structural constraints. Even when the error associated with the tensor characterization is taken into account, the accuracy of these constraints is far greater than the more familiar distance constraints of solution NMR methodology. Solid-state NMR is not an ideal method for determining global conformations, but it can provide structural detail of ultrahigh resolution for a few sites. Here the orientation of the indole rings in the gramicidin channel conformation is determined with respect to the channel axis at a higher level of resolution than has even been achieved before for a bilayer bound peptide or protein. The two independent approaches for determining the orientation of the Trp_{11} ring, resulted in structures that agreed within 3.7° and the two approaches were in no way refined. In fact, the refinement of data with such small error bars generates a major challenge for the computationalist when the data overdetermines the orientation of the site.

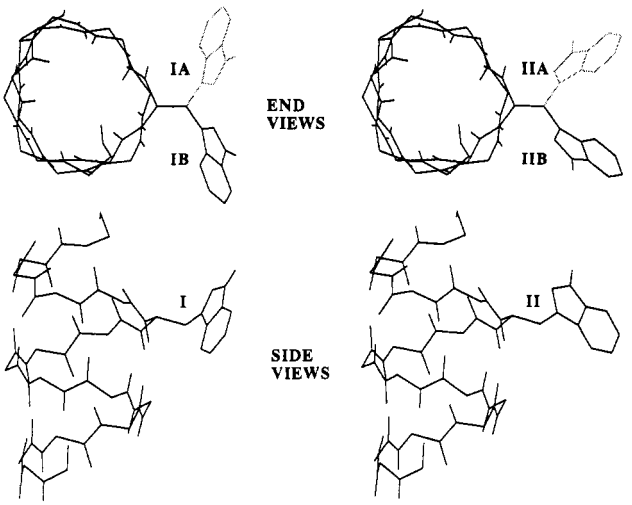

FIGURE 10: The four possible conformations for Trp_{11}. Both side and end views are shown for a gramicidin monomer in the channel conformation. The χ_1, χ_2 angles for these conformers are as follows: IA, 172°, 86°; IB, 283°, 274°; IIA, 172°, 28°; IIB, 283°, 332°. The difference between IA and IB and between IIA and IIB represent mirror images about the plane formed by the magnetic field direction and the C_α–C_β bond vector. The difference between class I and II conformations represents only a change in χ_2 and a mirror image about the plane formed by the magnetic field direction and the C_β–C_γ bond vector. Only the class I conformers are consistent with the Raman results.

The four conformations for each indole are shown by example in Figure 10. Conformers IA and IB represent images about a mirror plane formed by the C_α–C_β bond and the magnetic field direction, and therefore, in the side view shown these two conformers are superimposable. Similarly, conformers IIA and IIB are different images about the same plane, and the side-view projection again represents the superposition of two conformers. The difference between conformation I and II is a change only in χ_2. There is evidence from Raman studies that the χ_2 values for each of the tryptophans is ±90° in gramicidin (Takeuchi et al., 1990), and therefore the two conformers, IA and IB, are favored which have χ_2 angles of ±82° to ±93° versus conformations and IIA and IIB that have χ_2 angles of ±28° to ±40° for the different indole sites. However, these Raman studies were performed on gel-phase lipids, and there is some evidence (Scarlatta, 1988) that the tryptophan orientations change between liquid-crystalline and gel phase. Therefore, the Raman results must be considered with caution. The two conformers, IA and IB, have the indole rings packed against the polypeptide exterior, whereas IIA and IIB have the indole rings radiating from the channel axis.

The orientation of the indoles with respect to the channel axis is potentially very uniform and therefore supports the conclusion of the electrophysiologists (Becker et al., 1991) who noted that the incremental replacement of tryptophan residues by phenylalanine results in a regular incremental decrease in conductance. Each of the indoles are also oriented so that they could hydrogen bond with solvent or lipid at the hydrophobic–hydrophilic interface as in Figure 11 (Lazo et al., 1992; Meulendijks et al., 1989; O'Connel et al., 1990). For decades specific protein–lipid interactions have been sought. It appears that the tryptophans have at least two very significant roles for this cation channel. First, they stabilize the gramicidin monomer in the lipid monolayer. Gramicidin A added to one side of a lipid bilayer migrates very slowly to

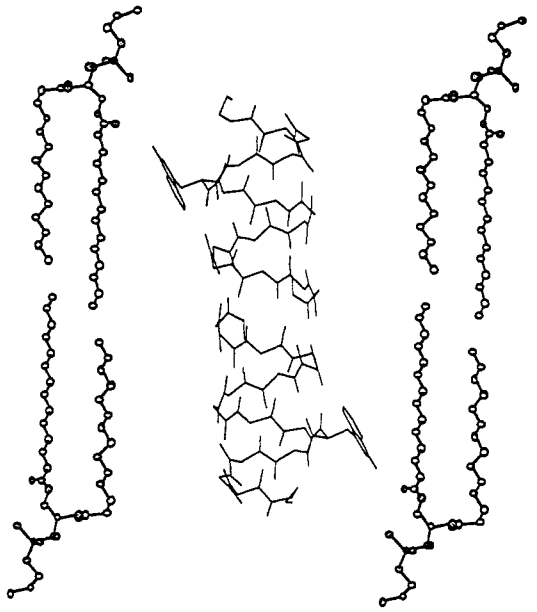

FIGURE 11: Backbone showing only the Trp_{11} sidechain and a single possible conformer, the orientation of the N–H bond toward the bilayer surface is shown. Such images suggest the possibility that the indole N–H groups may hydrogen bond with the fatty acyl carbonyl oxygens or with the hydrophilic bilayer interface.

the opposing monolayer, whereas gramicidin M^- in which the tryptophans have been uniformly replaced with phenylalanine much more readily migrates from one monolayer to the other (M. D. Becker and O. S. Andersen, personal communication). By forming hydrogen bonds with the hydrophilic surface of the bilayer the gramicidin monomer would be stabilized within a bilayer leaflet. Phenylalanine residues without such a propensity to form hydrogen bonds would permit ready migration of the monomer between leaflets. Similar indole and phenol orientations have been noted for other lipid bilayer bound proteins (Michel & Deisenhofer, 1990; Meers, 1990; Chattopadhyay & McNamee, 1991; Henderson et al., 1990; Weiss et al., 1991) and may be a general characteristic of membrane proteins.

The second role for tryptophan in gramicidin involves the role of the indole dipole moment on channel function. This dipole moment has been measured to be 2.08 D and it lies in the plane of the ring at an angle of 50° to the central $C_{\delta 2}$–$C_{\epsilon 2}$ bond (Weiler-Feichenfeld et al., 1970). As exemplified in Figure 12 and tabulated in Table V, the axial component of the dipole moment is larger than the perpendicular component. The uniformity in magnitude of the axial components, irrespective of conformer type and indole site, is striking. This correlates well with the incremental effect on channel conductance observed when indoles are replaced with phenyl groups one at a time (Becker et al., 1991). The orientation of the axial component is uniquely defined with the negative end of the dipole towards the channel center rather than channel entrance. Previous studies, such as Sancho and Martinez (1991), claimed that the ion–dipole interaction required to explain the conductance measurements on amino acid substituted gramicidins must have a dominant radial component to stabilize cations. While the radial component magnitudes are relatively small, the short interaction distance results in a significant energetic effect and the sign of the interaction for the most likely conformers (IA and IB) is such that cations will be stabilized in the channel. Even more significant may be the tangential component. If the cation moves on a helical path the ion could be affected by such a component.

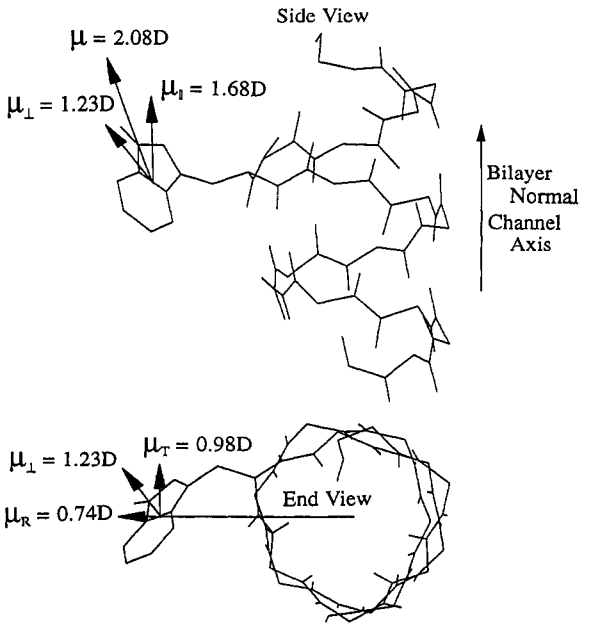

FIGURE 12: Analysis of the Trp_{11} dipole for the IA conformer. The magnitude of the dipole moment is 2.08 D. The $\mu_\parallel$ component is parallel with the channel axis and the bilayer normal. The $\mu_\perp$ component is perpendicular to the channel axis in the plane formed by μ and $\mu_\parallel$. The perpendicular component is broken down in the end view of the channel to show the radial and tangential components. The radial component is the same for the class I conformers, but the tangential component has the opposite direction for conformers IA and IB. The less likely class II conformers have different radial and tangential components, in fact, the sign of μ_R is opposite.

Table V: List of Dipole Moment Components for the Four Tryptophans of the Gramicidin Monomer

	Trp_9	Trp_{11}	Trp_{13}	Trp_{15}
$\mu_\parallel$ (D)[a]	+1.64	+1.68	+1.70	+1.72
$\mu_\perp$ (D)[b]	1.27	1.23	1.20	1.14

[a] Relative to the channel axis as diagramed in Figure 12. The sign of the $\mu_\parallel$ components is defined as positive when it points from the N to C terminal direction in a gramicidin monomer along positive Z direction. The magnitudes of $\mu_\parallel$ and $\mu_\perp$ are obtained from the orientationally constrained rings and independent of the backbone assumptions and therefore they are the same for each of the conformers. [b] Sign of $\mu_\perp$ components is unspecified.

The early models that were developed of the gramicidin channel had the indole rings of Trp_9 and Trp_{15} stacked (Venkatachalam & Urry, 1983). Because of the helical geometry such stacking requires that the plane of the two indole rings be approximately parallel with the bilayer surface. In the present study it is shown that the indole rings form a larger angle with the surface than in these model and consequently there is no evidence for ring stacking in the channel conformation above the gel to liquid crystalline phase transition temperature. However, it is not possible without an accurate backbone structure to yet say that there is absolutely no overlap between the Trp_9 and Trp_{15} indoles. Scarlatta (1988) in fluorescence studies presented evidence for base stacking of tryptophans below the phase transition, however, above the phase transition these studies showed no such evidence. The channel conformation is right-handed (Nicholson et al., 1989), and the left-handed conformations described by Venkatachalam and Urry (1983) and later used by many others have the indole N–H groups of Trp_{11} and Trp_{13} oriented toward the bilayer center. In this solid-state NMR study there is still structural ambiguity for the tryptophans, but the orientation of the indoles are uniquely

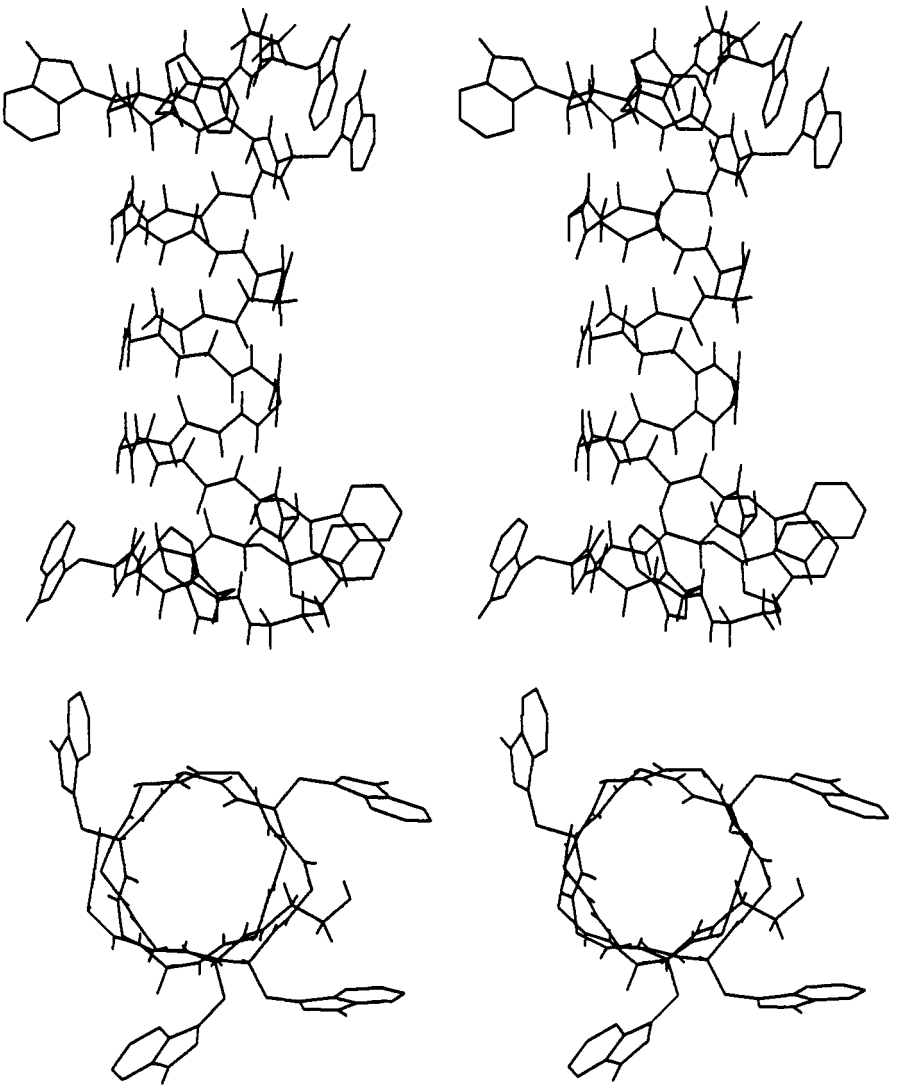

FIGURE 13: Stereoview of a possible channel conformation from both a side and end view. A model backbone structure is used and the χ_1 and χ_2 values for the tryptophans are as follows: Trp_9, 177°, 82°; Trp_{11}, 283°, 274°; Trp_{13}, 295°, 267°; Trp_{15}, 295°, 275°.

defined with respect to the bilayer and the N–H is toward the hydrophilic interface.

Many of the computational studies that have been performed in an effort to study the effect of the indole side chains on conformational stability (Meulendijks et al., 1989) and the energy profile for cation transport (Aqvist & Warshel, 1989; Etchebest & Pullman, 1985) have used the sidechain conformations of left-handed helical models such as Urry (1971) and Venkatachalam and Urry (1983). The helical sense has been shown to have a significant effect on sidechain conformation and the distance of residues from the bilayer surface, because the handedness effects the orientation of the C_α–C_β bonds. In general, the odd sites in the right-handed channel conformation are directed radially and somewhat towards the monomer–monomer junction. In a left-handed structure the C_α–C_β bonds for the odd sites are directed somewhat toward the bilayer surface. This has a significant effect on the χ values as well as the distance distribution for the indole N–H groups relative to the bilayer surface.

Etchebest and Pullman (1985) calculated the effects of individual tryptophans on the energy profile for cation transport. Trp_{13} was identified as having a prominent effect on the channel entrance energy profile. There is no evidence for uniqueness in the Trp_{13} site from Table V. Meulendijks et al. (1989) further refined a left-handed model in the presence of ester and ether linked lipids. The computational refinements maintained the stacking of Trp_9 and Trp_{15} and the incorrect orientation of Trp_{11} and Trp_{13}. Aqvist and Warshal (1989) found that the tryptophan orientation as described by Venkatachalam and Urry (1983) showed no significant effect on the energy profile.

The Arseniev model obtained from 2D NMR of SDS micelles is consistent with the set of possible indole orientations determined here. A consequence of the $N_{\epsilon 1}$–H bond orientations in SDS and in lipid bilayers shows very good agreement, although a 6° difference (Trp_9) corresponds to a 3-kHz difference in dipolar splitting which is greater than the experimental error. In particular, notice that the orientation of the N–H bonds show a clear trend toward a greater angle with respect to the channel axis for the sites closer to the bilayer surface. Possibly, the indole N–H bonds closer to the bilayer surface do not have to be oriented parallel with the channel axis to achieve hydrogen bonding with the hydrophilic interface. For the torsion angles of Trp_{13} and Trp_{15} the closest fit for the Arseniev model is within 7°, but it is as much as 33° off for Trp_9 and Trp_{11}. An error for the χ_1 and χ_2 angle determinations made here can be estimated from the Trp_{11} ring orientations that were determined by two independent methods. The root-mean-square difference for the C–H bond orientations was determined to be 3.7°. This value is used

here as an estimate of the orientational error bar. Therefore, a difference of 33° in χ_2 for Trp_{11} is far outside the margin of error and differences in several other torsion angles while smaller are likely to be significant.

All four of the indoles have a very similar orientation with respect to the bilayer surface and it is possible that they have very similar orientations with respect to the channel axis, but this latter conclusion has yet to be achieved. A possible set of indole orientations that is similar to Arseniev's conformation is shown in Figure 13. For the first time a calculation of the indole dipole moments has been achieved for the gramicidin channel and each of the tryptophan rings appear to be oriented so as to lower the central barrier of the energy profile and to stabilize the cations in the channel. Such structural details are necessary before the intricacies of channel function can be fully understood. For membrane bound polypeptides unique methods, such as solid-state NMR may be required to provide such detail.

ACKNOWLEDGMENT

The authors are indebted to the staff of the FSU NMR Facility: Joseph Vaughn, Richard Rosanske, and Thomas Gedris for their skillful maintenance, modification, and service of the NMR spectrometers and to Hank Henricks and Umesh Goli in the Bioanalytical Synthesis and Services Facility for their expertise and maintenance of the ABI 430A peptide synthesizer and HPLC equipment. The authors are indebted to Professors Benoit Roux and Eric Jakobsson for providing coordinates of their molecular dynamics refined conformational models and to Professor Arseniev for making available the coordinates of his solution NMR derived structure to the scientific community.

REFERENCES

Aqvist, J., & Warshel, A. (1989) *Biophys. J. 56*, 171–182

Arseniev, A. S., & Barsukov, V. F. (1986) in *Chemistry of Peptides and Proteins* (Voelter, W., Bayer, E., Ovchinnikov, Y. A., & Ivanov, V. T., Eds.) Vol. 3, pp 127–158, Walter de Gruyter & Co., Berlin.

Bamberg, E., Noda, K., Gross, E., & Lauger, P. (1976) *Biochim. Biophys. Acta 419*, 223–228.

Becker, M. D., Greathouse, D. V., Koeppe, R. E., II, & Andersen, O. S. (1991) *Biochemistry 30*, 8830–8839.

Bhat, T. N., Sasisekharan, V., & Vijayan, M. (1979) *Int. J. Peptide Protein Res. 13*, 170–184.

Brenneman, M. T., & Cross, T. A. (1990) *J. Chem. Phys. 92*, 1483–1494.

Chang, C., Waki, M., Ahmad, M., Meienhofer, J., Lundell, E. O., & Haug, J. D. (1980) *Int. J. Peptide Protein Res. 15*, 59–66.

Chattopadhyay, A., & McNamee, M. G. (1991) *Biochemistry 30*, 7159–7164.

Chiu, S.-W., Nicholson, L. K., Brenneman, M. T., Teng, Q., Subramanian, S., McCammon, J. A., Cross, T. A., & Jakobsson, E. (1991) *Biophys. J. 60*, 974–978.

Cornell, B. A., Separovic, F., & Smith, R. (1988) in *Transport Through Membranes: Carriers, Channels & Pumps* (Pullman, A., et al., Eds.) pp 289–295, Kluwer Academic Publishers, Dordrecht.

Cross, T. A., Ketchem, R. R., Hu, W., Lee, K.-C., Lazo, N. D., & North, C. L. (1992) *Bull. Magn. Reson. 14*, 96–101.

Cross, T. A., & Opella, S. J. (1982) *J. Mol. Biol. 159*, 543–549.

Cross, T. A., & Opella, S. J. (1983) *J. Am. Chem. Soc. 105*, 306–308.

Cross, T. A., & Opella, S. J. (1985) *J. Mol. Biol. 182*, 367–381.

Davis, J. H., Jeffrey, K. R., Bloom, M., Valic, M. I., & Higgs, T. P. (1976) *Chem. Phys. Lett. 42*, 390–394.

DiVerdi, J. A., & Opella, S. J. (1982) *J. Am. Chem. Soc. 104*, 1761–1762.

Etchebest, C., & Pullman, A. (1985) *J. Biomol. Struct. Dynam. 2*, 859–870.

Fields, C. G. (1989) M.S. Thesis, Florida State University, Tallahassee, FL.

Fields, G. B., Fields, C. G., Petefish, J., Van Wart, H. E., & Cross, T. A. (1988) *Proc. Natl. Acad. Sci. U.S.A. 85*, 1384–1388.

Fields, C. G., Fields, G. B., Noble, R. L., & Cross, T. A. (1989) *Int. J. Peptide Protein Res. 33*, 298–303.

Fletterick, R. J., Tsai, C.-C., & Hughes, R. E. (1971) *J. Phys. Chem. 75*, 918–922.

Haberkorn, R. A., Stark, R. E., van Willigen, H., & Griffin, R. G. (1981) *J. Am. Chem. Soc. 103*, 2534–2539.

Harbison, G., Herzfeld, J., & Griffin, R. G. (1981) *J. Am. Chem. Soc. 103*, 4752–4754.

Harbison, G., Jelinski, L. W., Stark, R., Torchia, D. A., Herzfeld, J., & Griffin, R. G. (1984) *J. Magn. Reson. 60*, 79–82.

Hartzell, C. J., Whitfield, M., Oas, T. G., & Drobny, G. P. (1987) *J. Am. Chem. Soc. 109*, 5966–5969.

Heitz, F., Spach, G., & Trudelle, Y. (1982) *Biophys. J. 39*, 87–89.

Henderson, R., Baldwin, J. M., Ceska, T. A., Zemlin, F., Beckmann, E., & Downing, K. H. (1990) *J. Mol. Biol. 213*, 899–929.

Hing, A. W., Adams, S. P., Silbert, D. F., & Norberg, R. E. (1990) *Biochemistry 29*, 4144–4156.

Hiyama, Y., Niu, C.-H., Silverton, J. V., Bavoso, A., & Torchia, D. A. (1988) *J. Am. Chem. Soc. 110*, 2378–2383.

Jacobs, R. E., & White, S. H. (1989) *Biochemistry 28*, 3421–3437.

Janin, J., Wodak, S., Levitt, M., & Maigret, B. (1978) *J. Mol. Biol. 125*, 357–386.

Katsaras, J., Prosser, R. S., Stinson, R. H., & Davis, J. H. *Biophys. J. 61*, 827–830.

Killian, J. A., Taylor, M. J., & Koeppe, II R. E. (1992) *Biochemistry 31*, 11283–11290.

Kimball, M. R., & Wallace, B. A. (1981) *Acta Crystallogr., Sec. A 37*, c50.

Kinsey, R. A., Kintanar, A., & Oldfield, E. (1981) *J. Biol. Chem. 256*, 9028–9036.

Kvick, A., Al-Karaghouli, A. R., & Koetzle, T. F. (1977) *Acta Crystallogr. B33*, 3796–3801.

Langs, D. A., Smith, G. D., Courseille, C., Precigoux, G., & Hospital, M. (1991) *Proc. Natl. Acad. Sci. U.S.A. 88*, 5345–5349.

Lazo, N. D., Hu, W., & Cross, T. A. (1992) *J. Chem. Soc., Chem. Commun.* 1529–1531.

LoGrasso, P. V., Nicholson, L. K., & Cross, T. A. (1989) *J. Am. Chem. Soc. 111*, 1910–1912.

Lomize, A. L., Orechov, V. Yu., & Arseniev, A. S. (1992) *Bioorg. Khim. 18*, 182–200.

Macdonald, P. M., & Seelig, J. (1988) *Biochemistry 27*, 2357–2364.

McGregor, M. J., Islam, S. A., & Sternberg, M. J. E. (1987) *J. Mol. Biol. 198*, 295–310.

Mai, W., Hu, W., Wang, C., & Cross, T. A. (1993) *Protein Sci. 2*, 532–542.

Meers, P., (1990) *Biochemistry 29*, 3325–3330.

Meulendijks, G. H. W. M., Sonderkamp, T., Dubois, J. E., Nielsen, R. J., Kremers, J. A., & Buck, H. M. (1989) *Biochim. Biophys. Acta 979*, 321–330.

Michel, M., & Deisenhofer, J. (1990) *Curr. Top. Membr. Trans. 36*, 53–69.

Munowitz, M., Aue, W. P., & Griffin, R. G. (1982) *J. Chem. Phys. 77*, 1686–1689.

Nicholson, L. K., & Cross, T. A. (1989) *Biochemistry 28*, 9379–9385.

Nicholson, L. K., LoGrasso, P. V., & Cross, T. A. (1989) *J. Am. Chem. Soc. 111*, 400–401.

Nicholson, L. K., Teng, Q., & Cross, T. A. (1991) *J. Mol. Biol. 218*, 621–637.
Oas, T. G., Hartzell, C. J., Dahlquist, F. W., & Drobny, G. P. (1987) *J. Am. Chem. Soc. 109*, 5962–5966.
O'Connell, A. M., Koeppe, R. E., II, & Andersen, O. S. (1990) *Science 250*, 1256–1259.
Pake, G. E. (1948) *J. Chem. Phys. 16*, 327–336.
Ponder, J. W., & Richards, F. M. (1987) *J. Mol. Biol. 193*, 775–791.
Roberts, J. E., Harbison, G. S., Munowitz, M. G., Herzfeld, J., & Griffin, R. G. (1987) *J. Am. Chem. Soc. 109*, 4163–4169.
Sancho, M., & Martinez, G. (1991) *Biophys. J. 60*, 81–88.
Scarlatta, S. F. (1988) *Biocphys. J. 54*, 1149–1157.
Scarlatta, S. F. (1991) *Biochemistry 30*, 9853–9859.
Seelig, J., & Macdonald, P. M. (1987) *Acc. Chem. Res. 20*, 221–228.
Separovic, F., Hayamizu, K., Smith, R., & Cornell, B. A. (1991) *Chem. Phys. Lett. 181*, 157–162.
Smith, R., & Cornell, B. A. (1986) *Biophys. J. 49*, 117–118.
Subramanian, E., & Sahayamary, J. J. (1989) *Int. J. Peptide Protein Res. 34*, 134–138.
Takeuchi, H., Nemoto, Y., & Harada, I. (1990) *Biochemistry 29*, 1572–1579.
Teng, Q. (1990) Ph.D. Dissertation, Florida State University.
Teng, Q., & Cross, T. A. (1989) *J. Magn. Reson. 85*, 439–447.
Teng, Q., Nicholson, L. K., & Cross, T. A. (1991) *J. Mol. Biol. 218*, 607–619.
Teng, Q., Iqbal, M., & Cross, T. A. (1992) *J. Am. Chem. Soc. 114*, 5312–5321.
Urry, D. W. (1971) *Proc. Natl. Acad. Sci. U.S.A. 68*, 672–676.
Venkatachalam, C. M., & Urry, D. W. (1983) *J. Comput. Chem. 5*, 64–71.
Wallace, B. A., & Janes, R. W. (1991) *J. Mol. Biol. 217*, 625–627.
Wang, C., Teng, Q., & Cross, T. A. (1992) *Biophys. J. 61*, 1550–1556.
Weiler-Feilchenfeld, H., Pullman, A., Berthod, H., & Giessner-Prettre, C. (1970) *J. Mol. Struct. 6*, 297–304.
Weiss, M. S., Abele, U., Weckesser, J., Welte, J., Schiltz, E., & Schulz, G. E. (1991) *Science 254*, 1627–1630.